Magazine of Civil Engineering. 2019. 90(6). Pp. 62–71
Инженерно-строительный журнал. 2019. № 6(90). С. 62–71

Magazine of Civil Engineering

ISSN 2071-0305

journal homepage: http://engstroy.spbstu.ru/

DOI: 10.18720/MCE.90.6

Behavior of two-way slabs subjected to drop-weight

R. Al-Rousan*
Jordan University of Science and Technology, Irbid, Jordan
** E-mail: rzalrousan@just.edu.jo*

Keywords: engineering, materials science, technology, civil engineering, structural concrete

Abstract. Prediction of punching shear strength in RC two-way slabs with different fiber volume fractions, and freely drop weight heights (Impact load) is fundamental to propose structural design procedures for structures subjected to impact load. Moreover, the punching failure of two-way slabs subjected to impact can consider as a complex behavior in design. Thus, the punching shear capacity of reinforced concrete (RC) two-way slabs subjected to drop-weight impacts investigated in this paper by using Nonlinear Finite Element Analysis (NLFEA). Firstly, the simulated models were validated against fifteen RC slabs with Polypropylene Fiber (PF) volume (V_f) of 0, 0.3, 0.6, and 0.9 % and subjected to impact load at the height of 0, 1.2, and 2.4 m. Then, the simulated slabs were expanded to cover slabs not subjected to impact load (impact height (H_I) of 0 m) and slabs with V_f of 0 % to 1.2 % and subjected to impact load at the height of 1 m to 11m, resulting in a total of 182 RC slabs. The behavior of each slab evaluated in terms of the crack patterns, ultimate punching shear capacity, and deflection profile. The results showed that adding the PF at a dosage of 0.1 to 1.2 % by volume of concrete leads to significant enhancement in the overall structural behavior of the slabs and their resistance to impact loading. Attractively, after impact height of 10 m (KE = 686.00 J), the simulated RC slabs with PF volume fraction less than 0.7 % are failed. While all the simulated RC slabs subjected to impact load at the height of 11 m (KE 754.26 J) failed. Finally, NLFEA was also performed to provide a prediction for impact factor based on PF volume fraction and the impact load height.

1. Introduction

The response of reinforced concrete (RC) elements subjected to impact load is a hot topic in the previously published research work. Also, it still needs more elaboration to understand their complex behavior. This hot topic is significant especially in the area of RC nuclear facilities or military fortification structures that are used in high-hazard or high-threat applications as well as in the structures that are designed to resist the accidental impact loading due to falling rock and ship or vehicle collisions with offshore facilities, bridges, and buildings. Therefore, extensive work should be undertaken in an attempt to develop a design procedure for post-impact resistant and to improve the behavior of RC elements subjected to impact loads. Up to now, the establishing of empirical provisions for estimating the damage and structural capacity under specific impact loading is the most focused topic of the majority of the impact loading related research [1–8]. Nowadays two-way RC flat slabs can be considered as the excellent solution for residential, commercial, and office buildings because of the practical and economic issues such as the easy installation of electrical and mechanical infrastructures, the considerably simpler and reduced formwork, and faster site operations as well as the more comfortable and versatility space partitioning. Moreover, the punching failure considered as a complex behavior in the design of the RC two-way flat slab. Besides, the punching failure is typically brittle and considered as the ultimate load capacity of two-way RC slabs and can cause a sudden collapse of the entire structure [9–15].

Al-Rousan, R. Behavior of two-way slabs subjected to drop-weight. Magazine of Civil Engineering. 2019. 90(6). Pp. 62–71. DOI: 10.18720/MCE.90.6

Аль-Рушан Р. Поведение двухсторонних плит, подвергнутых падению груза // Инженерно-строительный журнал. 2019. № 6(90). С. 62–71. DOI: 10.18720/MCE.90.6

Recently, utilizing fiber reinforced concrete has emerged as a practical approach for enhancing the performance of RC elements under impact loading. Numerous studies have shown that FRC elements (conventional steel reinforcing bars) demonstrate superior resistances to global impact behavior than local damage mechanism development and. As a result, acquire enhanced energy absorption capabilities under impact loading concerning RC elements [16]. Also, FRC is used to increase the punching shear capacity and the deformation capacity of RC flat slabs due to the capability of fibers in the bridging after the creation of the cracks [17, 18]. Based on the previous literature review, the punching shear strength of the RC two-way flat slabs after impact load omitted. Therefore, this paper presents the methodology and conclusions from a nonlinear finite element analysis (NLFEA) program in terms of the effect of impact load on the punching shear behavior of RC and polypropylene fiber reinforced (PFR) concrete two-way slabs. Highlighting was placed on assessing the impact of fiber volume fractions, and freely dropped weight heights on the RC two-way flat slab behavior in terms of ultimate load capacity, deflection profile, toughness or energy absorption as well as the mode of failure.

2. Methods

2.1. Description of the experimental program

The experimental program reported by Al-Rousan [19] included testing fifteen two-way reinforced concrete slabs as a simply supported system with an equally clear length and width of 1.0 m as well as slab thicknesses of 7 cm. The investigated parameters include the slab thicknesses, ts (7 cm and 9 cm), fiber volume fractions (0 %, 0.3 %, 0.6 %, 0.9 %, and 1.2 %), and freely drop weight (10 cm in diameter and weighs 7 kg) heights, hi (0, 1.2 m, and 2.4 m). The slabs reinforced with seven steel bars with a diameter of 5 mm in each direction which is equivalent to steel reinforcement ratios of 0.0018 and 0.0025 for the 9 cm and 8 cm slabs according to the ACI 318-14 Code. A dropped mass height of 1.2 m and 2.4 m represented impact velocity of 4.85 m/s and 6.86 m/s, respectively, as well as the kinetic energy of 82.32 J and 164.64 J, respectively.

The RC two-way slabs were tested firstly under impact load by using a special design setup consists of steel members with I-section joined together to provide a horizontal platform to give simply supported condition for the two-way slab. A steel ball of 7 kg mass with adjustable heights of 1.2 m to 2.4 m is allowed to fall freely through 150 mm in diameter hollow tube member placed vertically to stick the top surface of the tested two-way slabs at the center. After applying the impact load, all slabs tested as simply supported in both directions placed and were monotonically loaded up to failure using a hydraulic jack centrally positioned at the top of the slab. A square steel plate with a thickness of 50 mm and a side length of 200 mm was used to simulate the column with 200 mm sides. The applied load measured by using the load cell. Three linear variable differential transformers (LVDT) were placed at a specific location to measure the deflection profile of the tested slabs. Figure 1 shows the stress-strain diagrams for the concrete batches with different fiber volume fractions as well as the compressive strength, splitting tensile strength, and modulus of elasticity. Table 1 shows the results of tested slabs

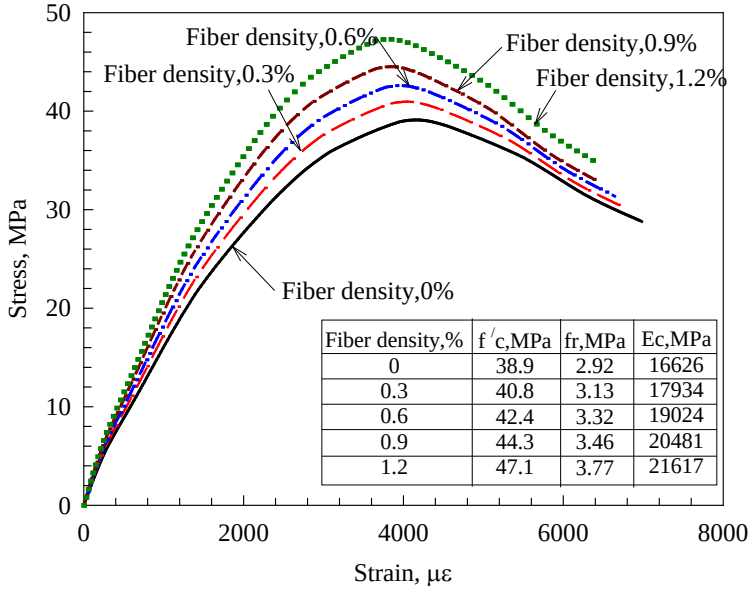

Fiber density,%	f ′c,MPa	fr,MPa	Ec,MPa
0	38.9	2.92	16626
0.3	40.8	3.13	17934
0.6	42.4	3.32	19024
0.9	44.3	3.46	20481
1.2	47.1	3.77	21617

Figure 1. Stress-strain diagrams and mechanical properties of concrete [19].

2.2. Nonlinear Finite Element Analysis

Nonlinear finite element (NLFEA) is a very useful and efficient tool for the analysis of complex structures in terms of the significant savings in the time, cost of fabrication and experimental testing, changing any parameter, allowing for obtaining the stress and corresponding strain, as well as the load capacity and corresponding displacement at any location. Accordingly, the NLFEA program package (ANSYS) was used to simulate the actual behavior of the tested RC slabs (Table 1). Then NLFEA simulation models (Table 2) were expanded to provide a parametric study of 182 RC slabs in terms of PF volume fraction (0.0–1.2 %) and impact load height (0 (No Impact) to 11 m (Failure of all slabs)) or kinetic energy (68.69 J and 754.26 J), respectively.

Table 1. Specimens' details and tested [19] versus NLFEA results.

Slab	Percent of fibers by volume (V_f)	Height of the falling mass (h_I), m	Experimental- Ultimate punching shear load, kN	NLFEA-Ultimate punching shear load, kN
Sf0.0t0.07h0	0		88.9	88.9
Sf0.3t0.07h0	0.30 %		93.4	93.4
Sf0.6t0.07h0	0.60 %	None	96.1	96.1
Sf0.9t0.07h0	0.90 %		100.7	100.7
Sf1.2t0.07h0	1.2 %		108.4	108.4
Sf0.0t0.07h1.2	0		61.8	62.0
Sf0.3t0.07h1.2	0.30 %		67.8	68.4
Sf0.6t0.07h1.2	0.60 %	1.2	74.9	73.7
Sf0.9t0.07h1.2	0.90 %		83.0	81.1
Sf1.2t0.07h1.2	1.2 %		91.0	91.5
Sf0.0t0.07h2.4	0		58.1	58.1
Sf0.3t0.07h2.4	0.30 %		63.9	64.1
Sf0.6t0.07h2.4	0.60 %	2.4	70.4	69.2
Sf0.9t0.07h2.4	0.90 %		77.9	76.0
Sf1.2t0.07h2.4	1.2 %		85.5	85.8

Table 2. NLFEA RC slabs details and ultimate load capacity.

Impact Load		V_f, %												
H_I, m	KE, J	0.0	0.1	0.2	0.3	0.4	0.5	0.6	0.7	0.8	0.9	1.0	1.1	1.2
0.0	**0.00**	**88.9**	91.0	92.4	**93.4**	94.3	95.1	**96.1**	97.3	98.8	**100.7**	102.9	105.5	**108.4**
1.0	68.69	63.5	66.0	68.1	70.0	71.8	73.6	75.5	77.7	80.2	83.0	86.2	89.8	93.8
1.2	**82.33**	**62.0**	64.5	66.5	**68.4**	70.1	71.8	**73.7**	75.9	78.3	**81.1**	84.2	87.7	**91.5**
2.0	137.16	61.0	63.4	65.4	67.2	68.9	70.7	72.5	74.6	77.0	79.7	82.8	86.2	90.0
2.4	**164.71**	**58.1**	60.4	62.4	**64.1**	65.7	67.4	**69.2**	71.1	73.4	**76.0**	78.9	82.2	**85.8**
3.0	205.90	56.8	59.0	60.9	62.6	64.2	65.8	67.5	69.4	71.7	74.2	77.1	80.3	83.8
4.0	274.13	52.9	55.0	56.7	58.3	59.8	61.3	62.9	64.7	66.8	69.1	71.8	74.8	78.1
5.0	343.04	48.2	50.1	51.7	53.1	54.5	55.8	57.3	59.0	60.9	63.0	65.4	68.2	71.2
6.0	411.27	43.5	45.2	46.7	48.0	49.2	50.4	51.8	53.2	54.9	56.9	59.1	61.6	64.3
7.0	479.93	38.4	39.9	41.2	42.3	43.4	44.5	45.7	47.0	48.5	50.2	52.2	54.3	56.7
8.0	548.63	29.3	30.4	31.4	32.3	33.1	33.9	34.8	35.8	37.0	38.3	39.7	41.4	43.2
9.0	617.25	13.2	13.7	14.1	14.5	14.9	15.3	15.7	16.1	16.6	17.2	17.9	18.6	19.4
10.0	686.00	F	F	F	F	F	F	F	0.9	2.4	4.2	6.5	9.1	11.9
11.0	754.26	F	F	F	F	F	F	F	F	F	F	F	F	F

N o t e : H_i: V_f: Percent of fibers by volume Impact load height, KE: Kinetic Energy, and F: Failure.

The SOLID65 element is capable of predicting the non-homogeneity, brittleness, and nonlinear behavior of concrete materials using a smeared crack approach with ultimate uniaxial tensile and compressive strengths (Figure 1). The detailed concrete properties in tension, compression, and modulus of elasticity are included earlier in Section 2.1. The Poisson's ratio is taken as 0.2. The shear transfer coefficient (β_t) taken as 0.8, which is nearly more than typical values for plain concrete since the fibers allow for the transfer of stress across the cracks. The efficiency of the PF in increasing the tensile and flexural strengths of the concrete based on the number and the orientation of PF per unit cross-sectional concrete area evaluated. The amount and orientation of PF per unit area were calculated based on the probability method proposed by Parviz and Lee [20]. LINK8 element was used to simulate the steel reinforcement bars with elastic-perfectly plastic behavior, Poisson's ratio of 0.3, yield strength of 460 MPa, and elastic modulus of 200 GPa. The Steel ball, steel plates at the loading and support locations were simulated using the SOLID45 element with linear elastic behavior; Poisson ratio and elastic modulus of 0.3 and 200 GPa, respectively.

Figure 2 shows the typical NLFEA meshing of the RC slab before and after the impact load. In NLFEA, the total applied load divided into a series of load steps or load increments. Newton-Raphson equilibrium iterations

provide convergence at the end of each load increment within tolerance limits equal five times the default tolerance limits of 0.5 % and 5 % for force and displacement checking to achieve the convergence of NLFEA solution.

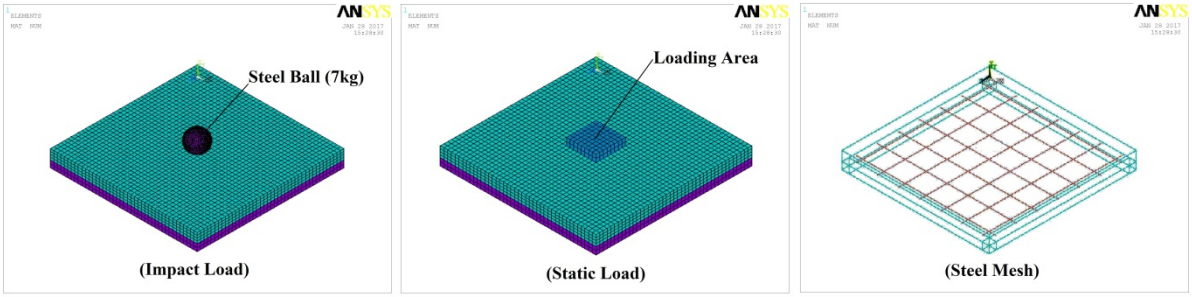

Figure 2. Typical finite element meshing of the RC slabs before and after impact.

3. Results and Discussion

3.1. Validation of NLFEA results

The tested RC slabs were simulated to validate the NLFEA, as shown in Table 2. The results from the experimental and NLFEA compared in terms of the load-deflection curves (Figure 3) and the ultimate load at failure (Table 2). Inspection of Figure 3 reveals that the NLFEA load-deflection curves had an excellent agreement with the experimental results. Moreover, Table 2 indicates that the NLFEA simulated RC slabs are very close to the tested ones in terms of the load-deflection behavior (Figure 3), ultimate load capacity (Table 2), and mode of failure (Figure 4).

For further illustration, the NLFEA models were expanded to cover the effect of PF volume fraction and impact load height or kinetic energy on the impact factor (b). Impact factor (b) calculated by dividing the ultimate load capacity of the slab subjected to impact load by the control slab (no impact) as shown in Table 3. Depending on the kinetic energy of the RC slabs having similar concrete compressive and tensile strength, Table 3 can be utilized to predict the required impact factor of a specific PF volume fraction. After an impact height of 10 m (KE = 686.00 J), the simulated RC slabs with PF volume fraction less than 0.7 % failed. While all the simulated RC slabs subjected to impact load at the height of 11 m (KE 754.26 J) failed.

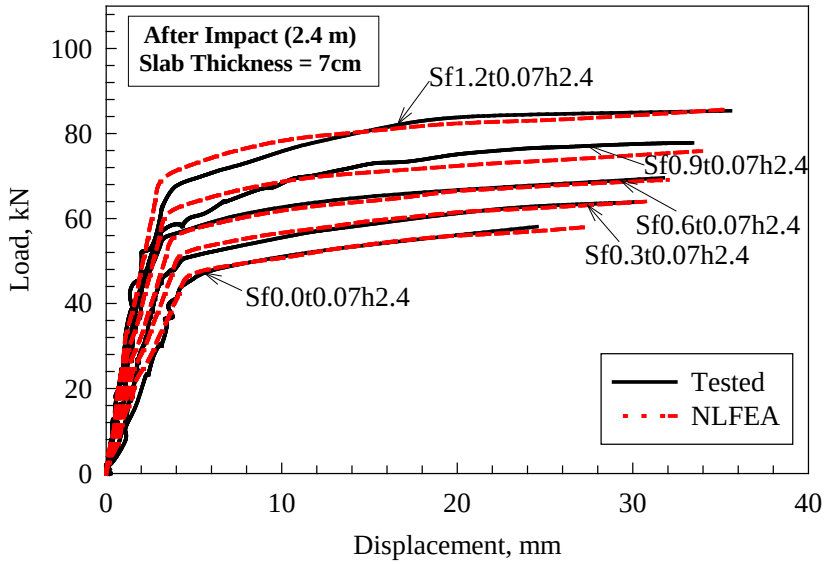

Figure 3. Typical tested [19] and NLFEA Load versus mid-span displacementcurves.

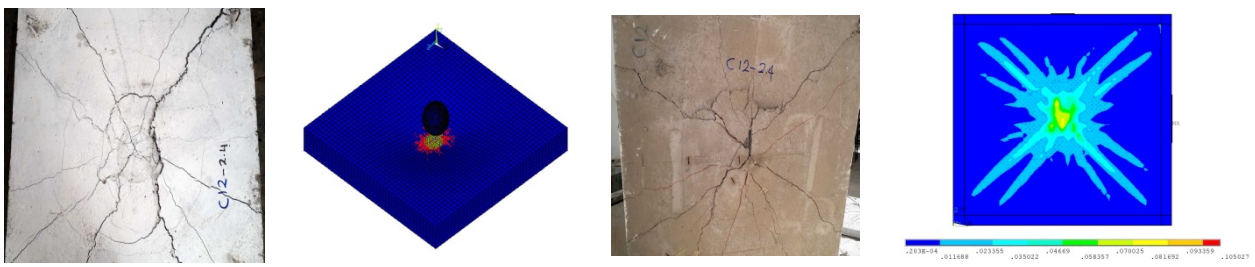

Sf0.6t0.07h2.4 (Top-Crack patterns) – 7 cm Sf0.6t0.07h2.4 (Bottom-strain contours) – 7 cm

Figure 4. Typical tested [19] and NLFEA results of RC slabs.

Table 3. Impact factor (b) using NLFEA.

Impact Load		b												
H_I, m	KE, J	0.0	0.1	0.2	0.3	0.4	0.5	0.6	0.7	0.8	0.9	1.0	1.1	1.2
0.0	0.00	1.000	1.000	1.000	1.000	1.000	1.000	1.000	1.000	1.000	1.000	1.000	1.000	1.000
1.0	68.69	0.714	0.726	0.738	0.749	0.762	0.774	0.786	0.799	0.812	0.825	0.838	0.852	0.866
1.2	82.33	0.697	0.709	0.720	0.732	0.743	0.755	0.768	0.780	0.793	0.805	0.818	0.832	0.845
2.0	137.16	0.686	0.697	0.708	0.720	0.731	0.743	0.755	0.767	0.779	0.792	0.805	0.818	0.831
2.4	164.71	0.654	0.664	0.675	0.686	0.697	0.708	0.720	0.731	0.743	0.755	0.767	0.780	0.792
3.0	205.90	0.638	0.649	0.659	0.670	0.680	0.691	0.703	0.714	0.725	0.737	0.749	0.761	0.773
4.0	274.13	0.595	0.604	0.614	0.624	0.634	0.644	0.655	0.665	0.676	0.687	0.698	0.709	0.721
5.0	343.04	0.542	0.551	0.560	0.569	0.578	0.587	0.597	0.606	0.616	0.626	0.636	0.646	0.657
6.0	411.27	0.489	0.497	0.505	0.513	0.522	0.530	0.539	0.547	0.556	0.565	0.574	0.584	0.593
7.0	479.93	0.432	0.439	0.446	0.453	0.460	0.468	0.475	0.483	0.491	0.499	0.507	0.515	0.523
8.0	548.63	0.329	0.334	0.340	0.345	0.351	0.357	0.362	0.368	0.374	0.380	0.386	0.393	0.399
9.0	617.25	0.148	0.151	0.153	0.155	0.158	0.160	0.163	0.166	0.168	0.171	0.174	0.177	0.179
10.0	686.00	F	F	F	F	F	F	F	0.009	0.024	0.042	0.063	0.086	0.110
11.0	754.26	F	F	F	F	F	F	F	F	F	F	F	F	F

N o t e : H_i: b: Impact factor, KE: Kinetic Energy, and F: Failure.

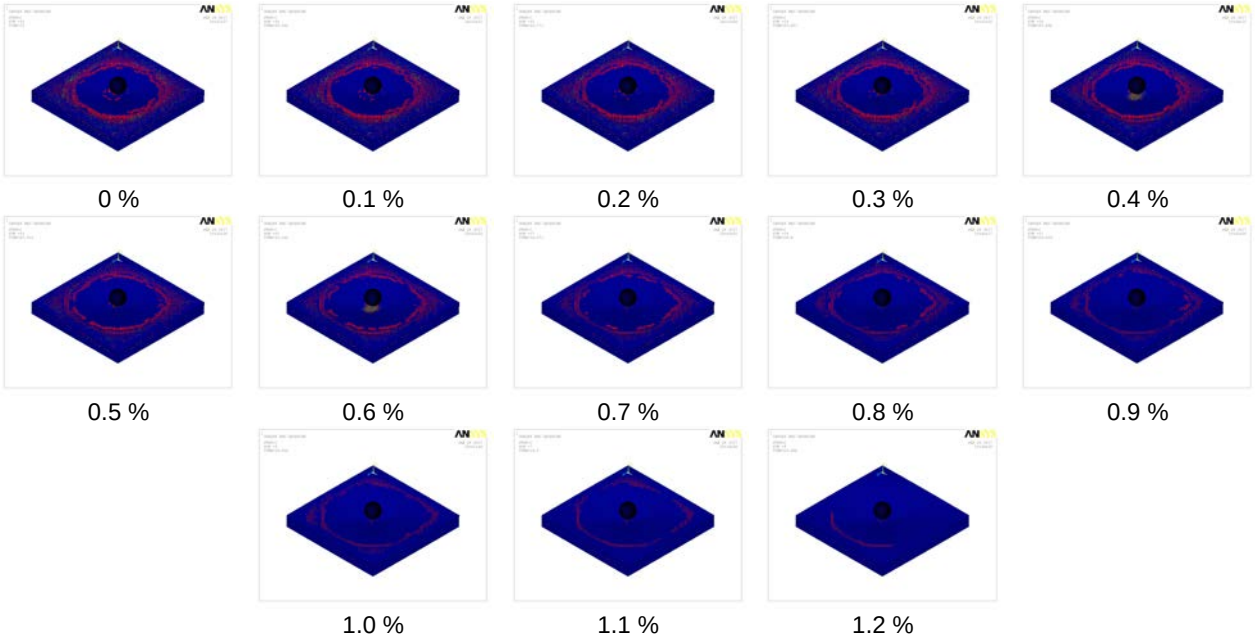

(a) Top Side

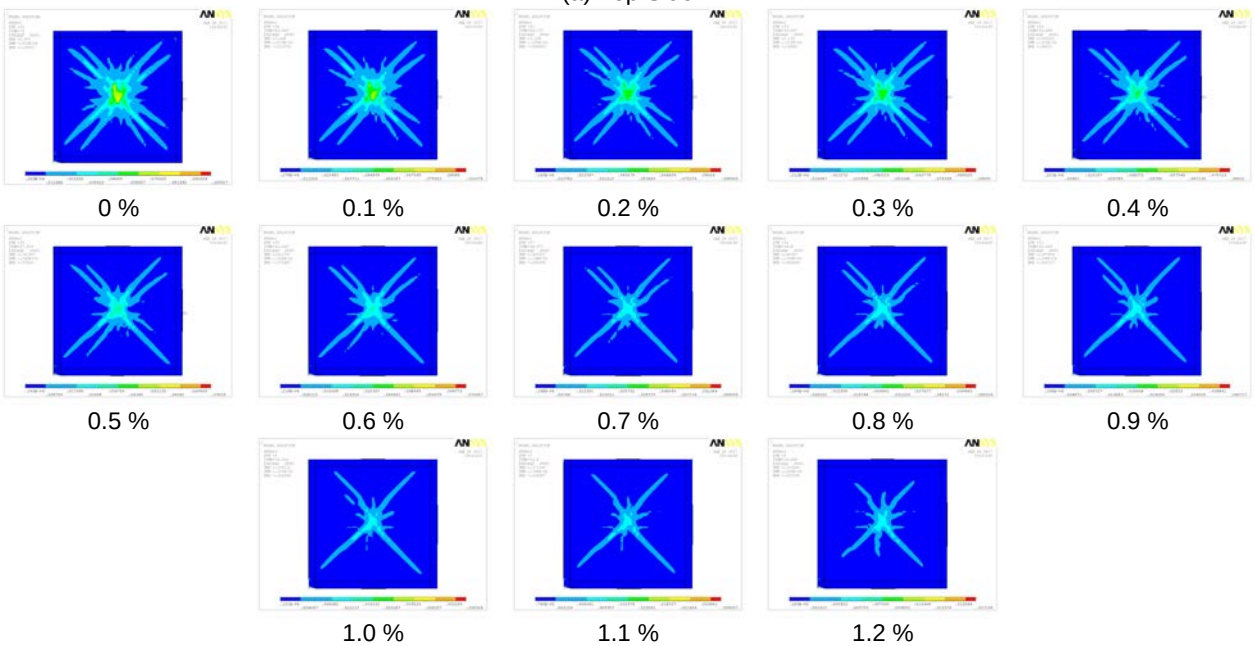

(b) Bottom Side

Figure 5. Typical crack patterns of the simulated models.

3.2. Mode of failure

Based on the NLFEA results, all simulated slabs failed in the punching shear mode, and flexural cracks started from the loading steel plate and extended until the edges of the tested slab. Punching shear mode of failure was a brittle that occurred near the loading steel plate (compression face or top surface) at the ultimate failure load. Followed by the development of a punching shear failure cone at the tensile face (Bottom surface). Figure 5 shows the typical punching shear failure on the compression face and tensile face. Inspection of Figure 5 shows that slabs subjected to impact had more flexural cracks and large punching shear cone than slabs not subjected to impact. Besides, Figure 5 shows the increase of fiber volume decreased the number of flexural cracks and the size of the punching shear cone. Because the fibers resist the applied forces until the fibers were pulled out from the concrete. Additionally, the occupation of fibers in stretching the failed bottom surface (tension face) of the slab away from the loading steel plate thus increased their punching shear capacity.

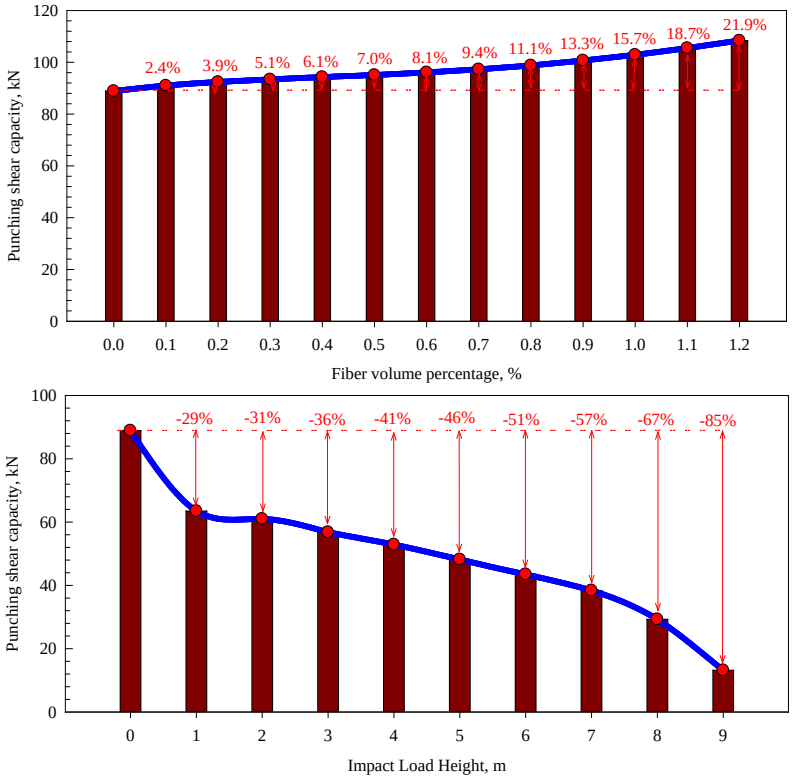

Figure 6. Effect of fiber volume percentage and impact load height on punching shear load.

3.3. Ultimate load capacity

Table 2 and Figure 6 show the summarized results and the effect of fiber volume percentage and impact load on the punching shear load of the tested slabs. Inspection of Figure 6 reveals that the ultimate punching shear capacity of control slab (slabs not subjected to impact) generally increases. Also, the degradation in slab strength due to impact load decreases with the increasing fiber volume percentage. Adding V_f in 0.1 to 1.2 % by volume fraction increased the ultimate punching capacity for slab without V_f by about 2.4 to 21.9 %, respectively. Also, the impact load at the height of 1 m to 9 m created degradation in the ultimate punching shear capacity of 29 % to 85 %, respectively. As well as the efficiency of fiber in absorbing of impact load or decreasing the ultimate load capacity degradation increased with the increasing of V_f percentage.

3.4. Load deflection behavior

Figure 7 shows the effect of the impact load and fiber volume on the load-displacement behavior, stiffness, and toughness. The stiffness defined as the slope of the curve from the initiation of the first crack (reaching the tensile strength of the concrete) to the displacement equal to 3 mm. The toughness defined as the area under the load-displacement behavior. The load-displacement behavior can be divided into two stages based on the crack growth and the shape of the load-displacement behavior, as shown in Figure 7. In the first stage (zero loadings to load at which the displacement equal to 3 mm), the behavior is approximately elastic liner before the initiation of the first crack (which is located at the center of the slab and close to the loading steel plate) and caused a reduction in the stiffness of the curve. Then, in the second stage, the stiffness was reduced suddenly, followed by the development of the punching shear cone. Inspection of Figure 7 reveals that the impact load height caused a higher reduction in stiffness and in toughness to control slab (no impact load) than fiber volume percentage. Besides, Figure 7 shows that the stiffness and toughness generally increase with the increasing fiber volume percentage. The adding of PFR assists in delaying and resisting the formulation and expanding of cracks, thus slab stiffness and toughness are

enhanced. Also, Figure 7 shows the proposed equation for predicting ultimate load capacity in terms of impact load height (Figure 7(a)) and fiber volume percentage (Figure 7(b)).

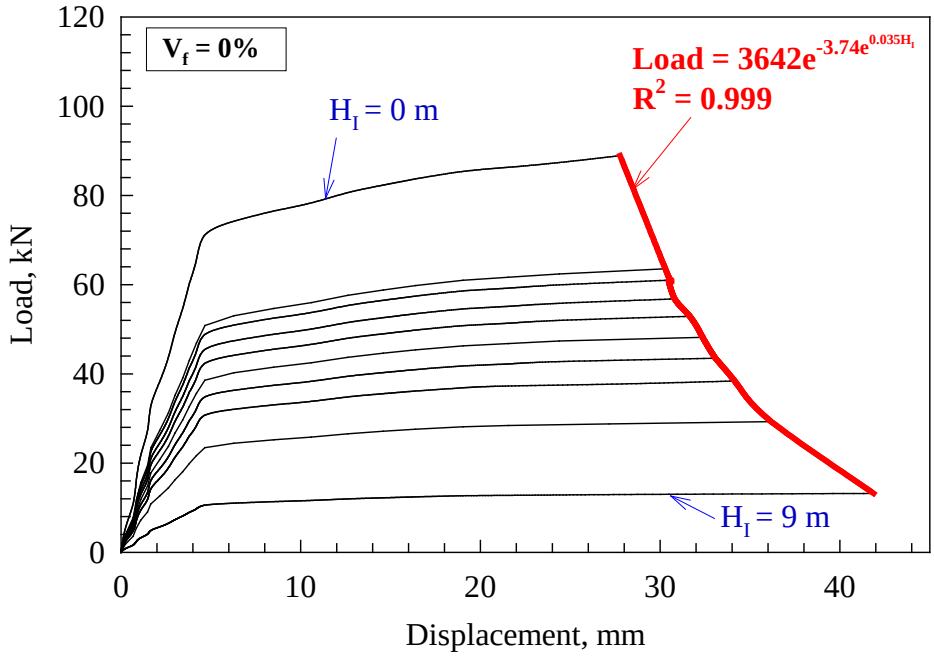

(a) Effect of impact load height (H_I)

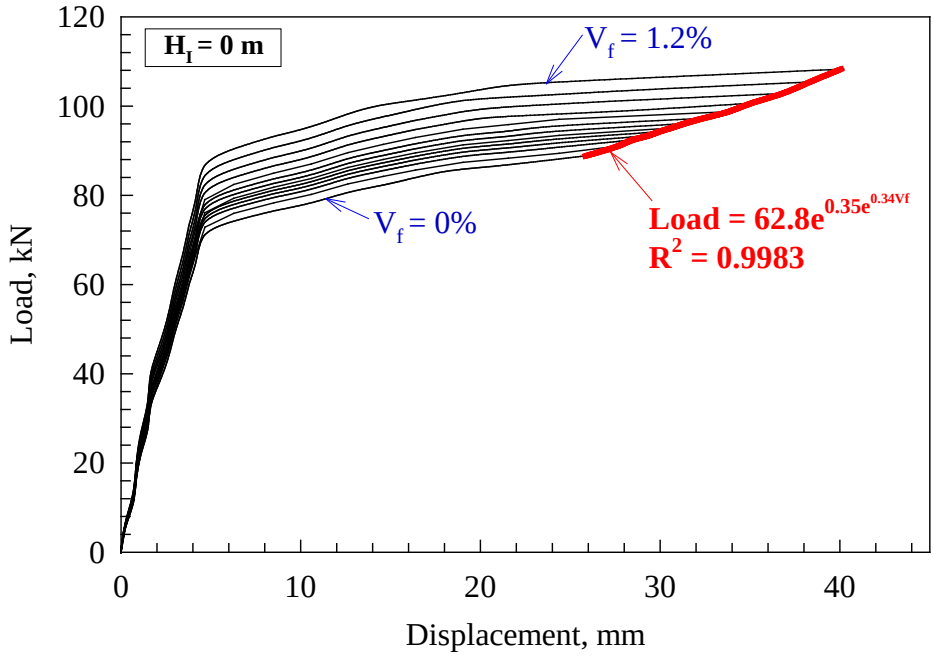

(b) Effect of fiber volume (V_f)

Figure 7. Typical load versus displacement curves.

3.5. Deflection profile

Assessment of the displacement profile of the simulated slabs provides further information (quantitative measure) on the topic of the effect of tested parameters (Figure 8). The global structural behavior that is not directly obvious from studying the load-displacement behavior and ultimate mid-point displacement. Figure 8 shows the effect of the impact load and fiber volume on the displacement profile. Inspection of Figure 8 reveals that the impact load height had the highest displacement profile, specifically at the mid-point comparing with the impact load at the lowest height. This mode of failure is observed the same in slabs subjected to impact at a higher height had more flexural cracks and large punching shear cone than slabs subjected to impact at the lowest height. While the displacement at the quarter-point is almost equal for both impact heights. It is seen that the PFR was successful in justifying the growth of localized failures in terms of the number of flexural cracks and the size of the punching shear cone. The PFR slabs exhibited displacement profile in which

displacement was more consistently distributed and, as a result, we're able to achieve more extensive displacement profile at failure.

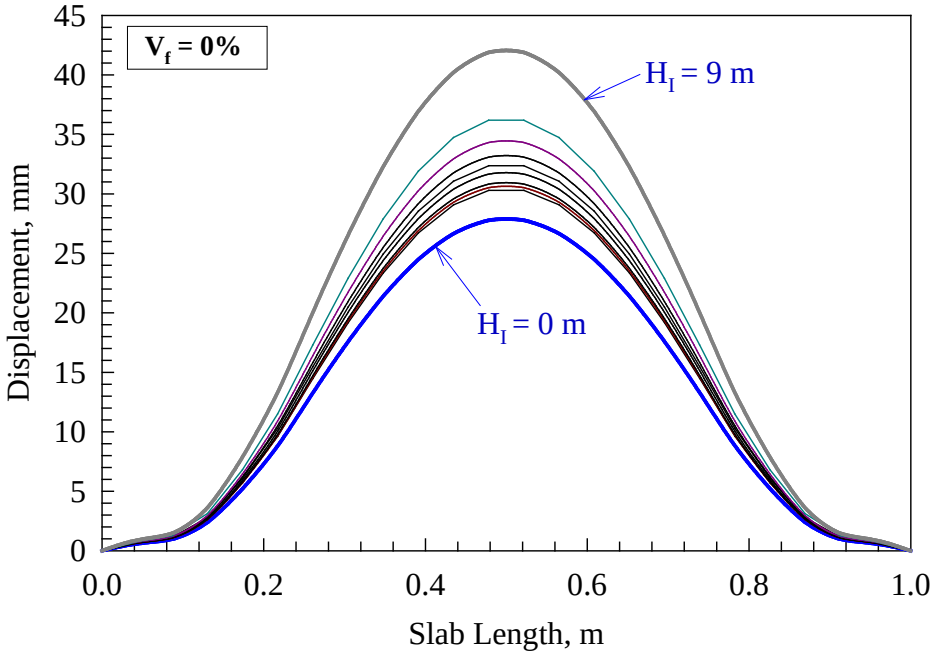

(a) Effect of impact load height (H_I)

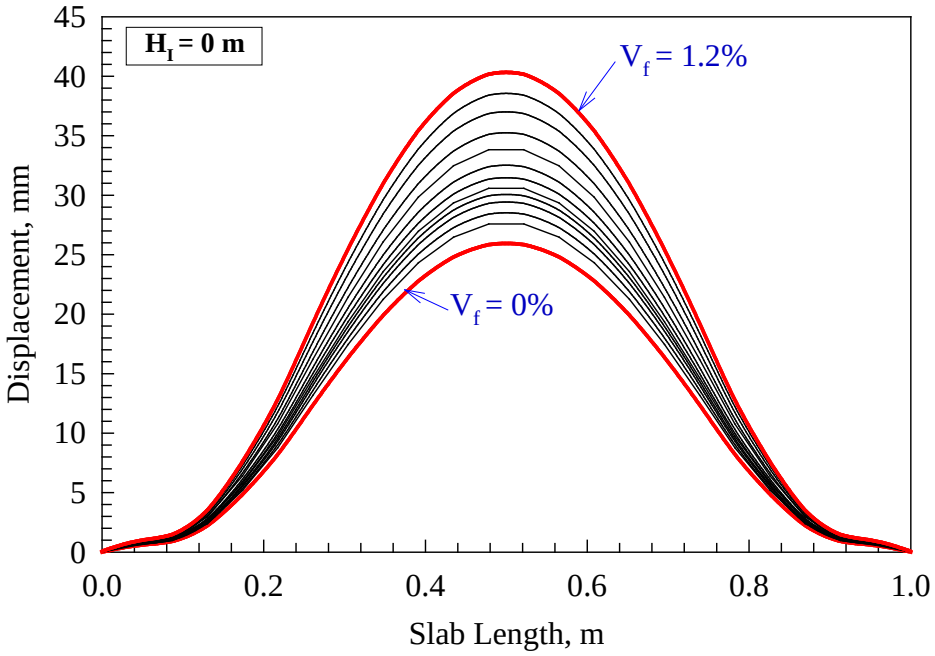

(b) Effect of fiber volume (V_f)

Figure 8. Typical displacement shapes,

3.6. Punching shear model for two-way RC slabs subjected to impact load

An empirical model was proposed to predict the punching shear strength of two-way RC slabs subjected to impact load as a function of tested parameters. Most models founded in the literature and design codes base their verifications on a critical section to find the punching shear strength of non-impacted RC slabs without shear reinforcement [9–20]. Equation (1) shows the ACI 318-14 expression for circular or square columns of two-way slab moderate relative to the concrete compressive strength and thickness of the slab.

$$V_R = 0.33 b_o d \sqrt{f_c'}, \quad (1)$$

where V_R is the punching shear capacity of two-way slabs at critical section located at $d/2$ from the face of the square or circular column;

d is the effective depth of the slab;

f'_c is the concrete compressive strength at 28 days;

b_o is the perimeter of the critical section.

Based on the above equation, Equation (2) can be used to describe the punching shear capacity of RC two-way slabs subjected to impact with some modifications as following:

$$V_R = \alpha\beta b_o d\sqrt{f'_c}, \tag{2}$$

where α and β is a factor accounting for fiber volume fraction and impact load effects, respectively. Based on the regression analysis of the RC two-way slabs not subjected to impact load (β = 1) as shown in Figure 9 [19], Equation (3) presents the relationship between the fiber volume fraction and α factor.

$$\alpha = 0.321e^{0.1523V_f}, \tag{3}$$

where V_f is the fiber volume fraction percentage. Based on the analysis of the RC two-way slabs subjected to impact load Table 3 shows the β factor based on impact height and fiber volume fraction percentage. Thus the punching shear strength of the RC two-way slabs subjected to impact can be defined by the following equations

$$V_R = (0.321\beta e^{0.1523V_f})b_o d\sqrt{f'_c}. \tag{4}$$

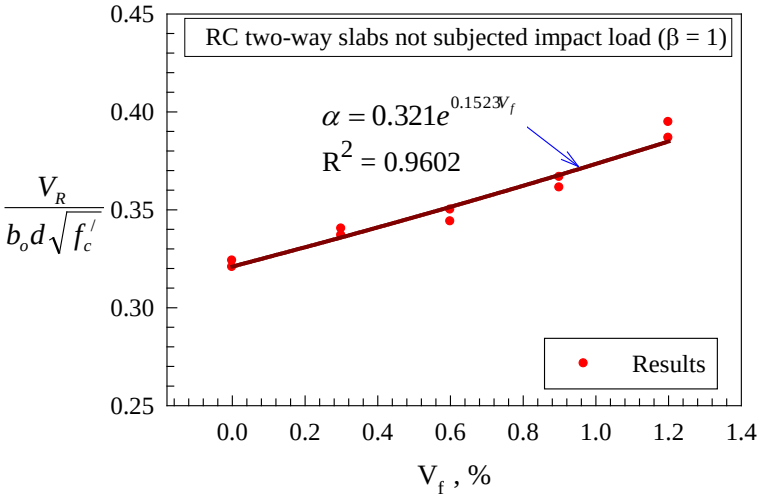

Figure 9. Relationships between fiber volume fraction percentage (V_f) and α factor for RC two way slabs not subjected impact load [19].

4. Conclusions

1. The increase in impact load and the fiber volume increased the number of flexural cracks and the size of the punching shear cone.

2. Adding fiber volume in 0.1 to 1.2 % by volume fraction enhanced the ultimate punching capacity with 2.4 to 21.9 % while the impact load at the height of 1 m to 9 m created degradation in the ultimate punching shear capacity of 29 % and 85 %.

3. After an impact height of 10 m, the simulated RC slabs with PF volume fraction less than 0.7 % failed. While all the simulated RC slabs subjected to impact load at the height of 11 m failed.

4. Based on innovative NLFEA verified with the experimental results, the impact factor (β) proposed for predicting the ultimate punching shear capacity of RC slabs at specific PF volume and kinetic energy.

5. Acknowledgments

The author acknowledges the technical support provided by the Jordan University of Science and Technology.

References

1. Kennedy, R.P.A. Review of Procedures for the Analysis and Design of Concrete Structures to Resist Missile Impact Effects. Nuclear Engineering and Design. 1976. 37(2). Pp. 183–203. DOI: 10.1016/0029-5493(76)90015-7.
2. Kishi, N., Mikami, J. Empirical Formulas for Designing Reinforced Concrete Beams under Impact Loading. ACI Structural Journal. 2012. 109(9). Pp. 509–519. DOI: 10.14359/51683870
3. Chen, Y., May, I.M. Reinforced Concrete Members under Drop Weight Impacts. Proceedings of the Institution of Civil Engineers Structures and Buildings. 2009. 162(1). Pp. 45–56. DOI: 10.1680/stbu.2009.162.1.45.
4. Hughes, G. Hard Missile Impact on Reinforced Concrete. Nuclear Engineering and Design. 1984. 77(1). Pp. 23–35. DOI: 10.1016/0029-5493(84)90058-X.
5. Sawamoto, Y., Tsubota, H., Kasai, Y., Koshika, N., Morikawa, H. Analytical Studies on Local Damage to Reinforced Concrete under Impact Loading by Discrete Element Method. Nuclear Engineering and Design. 1998. 179(2). Pp. 157–177. DOI: 0.1016/S0029-5493(97)00268-9.
6. Li, Q.M., Reid, S.R., Wen, H.M., Telford, A.R. Local Impact Effects of Hard Missiles on Concrete Targets. International Journal of Impact Engineering. 2005. 32(1–4). Pp. 224–284. DOI: 10.1016/j.ijimpeng.2005.04.005.
7. Saatci, S., Vecchio, F.J. Effects of Shear Mechanisms on Impact Behavior of Reinforced Concrete Beams. ACI Structural Journal. 2009. 106(1). Pp. 78–86. DOI: 10.14359/56286
8. Zamaliev, F.S., Zakirov, M.A. Stress-strain state of a steel-reinforced concrete slab under long-term. Magazine of Civil Engineering. 2018. 83(7). Pp. 12–23. DOI: 10.18720/MCE.83.2.
9. Tohid, Mousavi, Erfan, Shafei. Impact response of hybrid FRP-steel reinforced concrete slabs. Structures. 2019. 19. Pp. 436–448. DOI: 10.1016/j.istruc.2019.02.013.
10. Mastali, M., Ghasemi Naghibdehi, M., Naghipour, M., Rabiee, S.M. Experimental assessment of functionally graded reinforced concrete (FGRC) slabs under drop weight and projectile impacts. Construction and Building Materials. 2015. 95. Pp. 296–311. DOI: 10.1016/j.conbuildmat.2015.07.153.
11. Yilmaz, Tolga, Kirac, Nevzat, Anil, Özgür, Erdem, R. Tuğrul, Sezer, Ceyda. Low-velocity impact behaviour of two way RC slab strengthening with CFRP strips. Construction and Building Materials. 2018. 186. Pp. 1046–1063. DOI: 10.1016/j.conbuildmat.2018.08.027.
12. Wenjie, Wang, Nawawi, Chouw. Experimental and theoretical studies of flax FRP strengthened coconut fibre reinforced concrete slabs under impact loadings. Construction and Building Materials. 2018. 171. Pp. 546–557. DOI: 10.1016/j.conbuildmat.2018.03.149.
13. Kumar, Vimal, Iqbal, M.A., Mittal, A.K. Impact resistance of prestressed and reinforced concrete slabs under falling weight indenter. Procedia Structural Integrity. 2017. 6. Pp. 95–100. DOI: 10.1016/j.prostr.2017.11.015.
14. Lorena, Francesconi, Luisa, Pani, Flavio, Stochino. Punching shear strength of reinforced recycled concrete slabs. Construction and Building Materials. 2016. 127. Pp. 248–263. DOI: 10.1016/j.engstruct.2015.09.010
15. Micael M.G. Inácio, André F.O. Almeida, Duarte M.V. Faria, Válter J.G. Lúcio, António Pinho Ramos. Punching of high strength concrete flat slabs without shear reinforcement. Engineering Structures. 2015. 103. Pp. 275–284. DOI: 10.1016/j.engstruct.2015.09.010.
16. Zhang, J., Maalej, M., Quek, S.T. Performance of Hybrid- Fiber ECC Blast/Shelter Panels Subjected to Drop Weight Impact. Journal of Materials in Civil Engineering. ASCE. 2007. 19(10). Pp. 855–863. DOI: 10.1061/(ASCE)0899-1561(2007)19:10(855).
17. Cheng, M.Y., Parra-Montesinos, G.J. Evaluation of steel fiber reinforcement for punching shear resistance in slab–column connections – Part I: Monotonically increased load. ACI Structure Journal. 2010. 107(1). Pp. 101–109. DOI: 10.14359/51663394.
18. Maya, L.F., Fernández Ruiz, M., Muttoni, A., Foster, S.J. Punching shear strength of steel fibre reinforced concrete slabs. Engineering Structures. 2012. 40. Pp. 83–94. DOI: 10.1016/j.engstruct.2012.02.009.
19. Al-Rousan, R.Z. Failure Analysis of Polypropylene Fiber Reinforced Concrete Two-Way Slabs Subjected to Static and Impact Load Induced by Free Falling Mass. Latin American Journal of Solids and Structures. 2018. 15(1). Pp. e19. DOI: 10.1590/1679-78254895.
20. Parviz, S., Cha-Don, L. Distribution and orientation of fibers in steel fiber reinforced concrete. ACI Materials Journal. 1990. 87(5). Pp. 433–439. DOI: 10.14359/1803.

Contacts:

Rajai Al-Rousan, +962799887574; rzalrousan@just.edu.jo